

Concentration dependence of the transition temperature and isotope-effect exponent in high- T_c superconductors

É. A. Pashitskiĭ

Institute of Physics, Ukrainian Academy of Sciences, 252650 Kiev, The Ukraine

(Submitted 28 July 1993)

Pis'ma Zh. Eksp. Teor. Fiz. **58**, No. 5, 389–394 (10 September 1993)

The nonmonotonic concentration dependence which has been observed experimentally for the transition temperature T_c and the oxygen isotope-effect exponent α_0 can be explained by the model of a “plasmon” mechanism for superconductivity in a layered metal with a narrow 2D band near the Fermi level. The reasons are that this mechanism is invariant under a change in the sign of the charge carriers and that the plasma frequency of the “heavy” carriers is a nonmonotonic function of the extent to which the narrow band is filled. A possible explanation is proposed for the positive sign of the derivative of T_c with respect to the pressure in the new compound HgBaCaCuO with $T_c > 130$ K.

1. An empirical analysis of the behavior of T_c of various classes of layered metal–oxide cuprate compounds as a function of the number of dopant holes, x_p (or dopant electrons, x_n), in the primitive cell of the crystal per 2D conducting CuO_2 cuprate layer was carried out in Refs. 1–3. It was found that all these curves can be classified in one of two categories: Either they conform (completely or partially) to a “universal,” nearly symmetric, bell-shaped curve [this is true of, for example, p -type $\text{La}_{2-x}(\text{Ba,Sr})_x\text{CuO}_4$ in the interval $0.05 < xp < 0.27$ (Ref. 4) and n -type $\text{Nd}_{2-x}\text{Ce}_x\text{CuO}_4$ at $0.10 < x_n < 0.17$ (Ref. 5)], or they are asymmetric, with a rapid increase in T_c to a maximum value upon an increase or decrease in the hole density, followed by a transition to either a smoother, nonmonotonic T_c dependence or a nearly constant value of T_c [as in the layered BiSrCaCuO and TlBaCaCuO cuprates doped with Y, La, Pb, K, Na, etc., atoms^{1,3}]. For $\text{YBa}_2\text{Cu}_3\text{O}_{7-\delta}$ in the region $0 < \delta < 0.5$, the plot of T_c versus the oxygen content is typically “stepped.” The reason is the formation of an additional (third) cuprate layer with ordered 1D CuO chains at $\delta < 0.2$. As a result, there is uncertainty in a calculation of the number of holes (x_p) per layer.³

On the other hand, the concentration dependence of the oxygen isotope-effect exponent $\alpha_0 = -\frac{1}{2} \partial \ln T_c / \partial \ln M_0$ (M_0 is the mass of the oxygen atom) in cuprates of mixed composition $\text{Y}_{1-x}\text{Pr}_x\text{Ba}_{2-y}\text{Ca}_y\text{Cu}_3\text{O}_{7-\delta}$ (Ref. 7) and $\text{YBa}_{2-x}(\text{La, Sr})_x\text{Cu}_3\text{O}_{7-\delta}$ (Ref. 8) indicates that the isotope effect is suppressed as T_c increases. The suppression is such that α_0 reaches vanishing values near maximum T_c and even goes negative in the region of the decrease in T_c (see also Ref. 9). This behavior contradicts the well-known tendency of ordinary (low-temperature) superconductors with an electron–phonon coupling to exhibit a decrease in the isotope-effect exponent and a change in its sign with decreasing T_c .^{10,11} On the other hand, it correlates well with corresponding theoretical predictions of the behavior of T_c and

α_0 which were found in Ref. 12 on the basis of a model of the electron–plasmon interaction involving a hybridization of low-frequency acoustic plasmons with high-frequency optical phonons (oxygen vibrational modes). According to Ref. 13, on the other hand, in $\text{La}_{2-x}\text{Sr}_x\text{CuO}_4$ the oxygen isotope-effect exponent changes from anomalously large values $\alpha_0 \gtrsim 0.6$ near the point of structural instability of the lattice ($x_p \approx 0.13$), at which there is a sharp decrease in T_c ,^{14,16} to anomalously small but positive values $\alpha_0 \lesssim 0.1$ in the region of decreasing T_c ($0.15 < x_p < 0.27$).

In the present letter we show that the nonmonotonic concentration dependence of T_c observed in the superconducting metal–oxide cuprates, with corresponding correlations between T_c and α_0 , can be explained by the model of a “plasmon” mechanism for high- T_c superconductivity.¹²

2. According to the model¹² of a layered metal with a quasi-2D electron spectrum, with a broad band (of width $W_l \gtrsim 1$ eV) and a narrow one (of width $W_h \lesssim 0.1$ eV), which overlap near the Fermi level, the doping of the crystal involves primarily a filling of the narrow 2D band, with a high density of states and with a cosinusoidal spectrum in the strong-coupling approximation:

$$E_h(k_x, k_y) = \pm \left\{ E_0 + \frac{W_h}{2} \left[1 - \frac{1}{2} (\cos k_x a + \cos k_y a) \right] \right\}. \quad (1)$$

Here a is the lattice constant in the plane of the layers, and E_0 is the distance from the edge (top or bottom) of the broad band to the nearest edge of the narrow band ($E_0 < W_l/2$). As $T \rightarrow 0$, and as the narrow band becomes filled by nearly localized “heavy” (h) charge carriers, their density N_h and the Fermi energy $E_{Fh} \sim N_h$ initially increase. They reach a maximum at a half-filled band. The sign of the charge (the effective mass) of the h carriers then changes; as x_p (or x_n) increases, the values of N_h and E_{Fh} begin to decrease. They vanish when the band becomes completely filled. As was shown in Ref. 17, the plasma frequency of the h carriers, Ω_h , in a layered metal is

$$\Omega_h = \left\{ \frac{4e^2 W_h}{\pi \epsilon_\infty d} [E(\kappa_h) - (1 - \kappa_h^2)K(\kappa_h)] \right\}^{1/2}, \quad (2)$$

where

$$\kappa_h = \frac{2}{W_h} [E_{Fh}(W_h - E_{Fh})]^{1/2} \quad (0 \leq E_{Fh} \leq W_h/2), \quad (3)$$

ϵ_∞ is the optical dielectric constant of the crystal, d is the distance between conducting layers, and $K(\kappa_h)$ and $E(\kappa_h)$ are the complete elliptic integrals of the first and second kinds.

The solid curve in Fig. 1 shows the ratio Ω_h/Ω_h^{\max} versus $\mathcal{E}_h \equiv 2E_{Fh}/W_h$ for degenerate h carriers ($T=0$). This curve was found from (2) and (3) with $\Omega_h^{\max} = (4e^2 W_h/\pi \epsilon_\infty d)^{1/2} \lesssim 0.25$ eV at $W_h \lesssim 0.1$ eV, $\epsilon_\infty \gtrsim 4.5$, and $d \gtrsim 6 \text{ \AA}$.

At $T > E_{Fh}$, where the h carriers become nondegenerate, their plasma frequency depends on T and is given by¹⁷

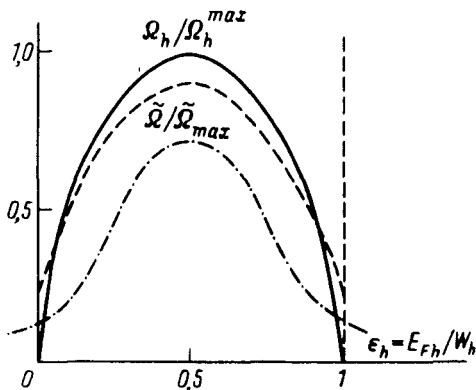


FIG. 1.

$$\Omega_h(T) = \left[\frac{\pi e^2 a^2 W_h}{\epsilon_\infty d} N_h(T) I_1 \left(\frac{W_h}{4T} \right) / I_0 \left(\frac{W_h}{4T} \right) \right]^{1/2}, \quad (4)$$

where

$$N_h(T) = \frac{2}{a^2} I_0^2 \left(\frac{W_h}{4T} \right) \exp \left\{ \left(\mu_h - E_0 - \frac{W_h}{2} \right) / T \right\}, \quad (5)$$

$I_0(z)$ and $I_1(z)$ are the Bessel functions of the first kind of imaginary argument, and μ_h is the chemical potential of the h carriers. This chemical potential is $\mu_h = E_{Fl} - E_0$ if the Fermi energy of the degenerate “light” (l) carriers in the wide 2D band satisfies $E_{Fl} \leq E_0 + W_h/2$, while it is $\mu_h = E_0 + W_h - E_{Fl}$ if $E_{Fl} > E_0 + W_h/2$. The dot-dashed curve in Fig. 1 shows $\Omega_h(T)$ for $T \neq 0$ as a function of the filling of the narrow 2D band for nondegenerate h carriers. This result was found from (4) and (5). We see that in this case $\Omega_h(T)$ does not vanish when the Fermi level is at the edges of or outside the narrow band, with $\mu_h \leq 0$.

At $T \gtrsim \mu_h$, at which the h carriers are described by Maxwell–Boltzmann statistics, their maximum 2D density at $E_0 \gg W_h/2$ is, according to (5), much smaller than the value ($\sim a^{-2}$) required for filling of the narrow 2D band. This result is in accordance with the Luttinger theorem for degenerate h carriers (heavy fermions).

On the other hand, the density (N_l) of l carriers in the wide 2D band, with the far lower density of states, and therefore the Fermi energy of these carriers, $E_{Fl} \sim N_l$, and the plasma frequency $\Omega_l \sim N_l^{1/2}$ remain nearly constant as the narrow band becomes filled as the doping proceeds. This conclusion is supported by experiment.^{18,19}

3. We will now show that with a “plasmon” superconductivity mechanism¹² a bell-shaped dependence of Ω_h on \mathcal{E}_h (Fig. 1) leads to the nonmonotonic behavior of T_c and α_0 as a function of the carrier density which is observed.

As was shown in Ref. 20, the nearly exact cancellation of the local-field effect and the strong-coupling effect in the case of Coulomb superconductivity mechanisms, in the case of a Cooper pairing of l carriers resulting from an exchange of virtual quanta of hybrid phonon–plasma oscillations in an ionic crystal,¹² even at fairly large values

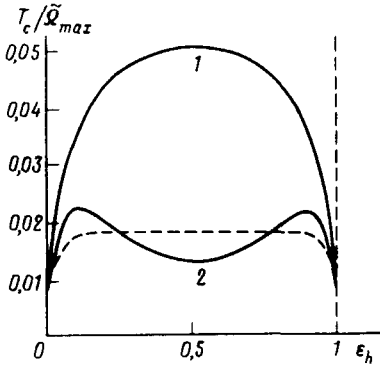


FIG. 2.

of the electron-plasmon coupling constant, $\lambda_{pl} \gtrsim 1$, means that we can estimate T_c from the exponential formula of the weak-coupling approximation:

$$T_c \approx \tilde{\Omega} \exp\{-1/[\lambda_{pl} - \mu_c^*(\tilde{\Omega})]\}, \quad (6)$$

where

$$\mu_c^*(\tilde{\Omega}) \approx \mu_c [1 + \mu_c \ln(E_{Fl}/\tilde{\Omega})]^{-1}, \quad \mu_c \approx \lambda_{pl}, \quad (7)$$

$$\tilde{\Omega} \approx [(\Omega_h^2 k_F d + \omega_{LO}^2)/(1 + \alpha_l)]^{1/2}, \quad \alpha_l = 1/k_F a_l^*. \quad (8)$$

Here $a_l^* = \epsilon_\infty/m_l^* e^2$ and $k_{Fl} = (2\pi N_l)^{1/2}$ are the first Bohr radius and the Fermi momentum of the l carriers, with an effective mass m_l^* and a 2D density N_l , and ω_{LO} is the frequency of longitudinal optical phonons, which correspond to vibrations of oxygen atoms in the conducting CuO_2 layers. The dashed curve in Fig. 1 shows the \mathcal{E}_h dependence of $\tilde{\Omega}$, i.e., the hybrid frequency of coupled acoustic plasmons and LO phonons, averaged over the Fermi surface of the l carriers, for the values $\alpha_l = k_{Fl} d = 1$, $\omega_{LO} = 400$ K, and $\Omega_h^{\max} = 1500$ K ($W_h = 0.05$ eV, $d = 12$ Å).

The solid curves in Fig. 2 show the ratio $T_c/\tilde{\Omega}_{\max}$ versus \mathcal{E}_h found for the case with a "pinning" of the Fermi level ($E_{Fl} \approx \text{const}$). The parameter values here are the same as in Fig. 1, with $\lambda_{pl} = \mu_c = 1$ and $E_{Fl} = 10\tilde{\Omega}_{\max}$ (curve 1) and $\lambda_{pl} = \mu_c = 0.7$ and $E_{Fl} = 4\tilde{\Omega}_{\max}$ (curve 2). The dashed curve shows $T_c(\mathcal{E}_h)/\tilde{\Omega}_{\max}$ for $\lambda_{pl} = \mu_c = 1$ and $E_{Fl} = 4\tilde{\Omega}_{\max}$.

Figure 3 shows the oxygen isotope-effect exponent $\alpha_0 = \partial \ln T_c / \partial \ln \omega_{LO}$ versus \mathcal{E}_h and T_c (here we are using $\omega_{LO} \propto M_0^{-1/2}$); these plots correspond to curves 1 and 2 in Fig. 2.

Finally, Fig. 4, from Ref. 3 shows experimental data on the density dependence of T_c for various cuprate compounds. We see that T_c remains essentially constant for $\text{YBa}_{2-x}\text{La}_x\text{Cu}_4\text{O}_8$ (triangles), $\text{Bi}_{1.8}\text{Pb}_{0.35}\text{Sr}_2\text{Ca}_2\text{Cu}_3\text{O}_{10+\delta}$ (filled diamonds), and $\text{Tl}_{0.5+x}\text{Pb}_{0.5-x}\text{Ca}_{1-y}\text{Y}_y\text{Sr}_2\text{Cu}_2\text{O}_7$ (filled circles) over a broad range of the hole density. In contrast, the curves of T_c versus x_p for $\text{Bi}_{1.8}\text{Pb}_{0.2}\text{Sr}_{1.6}\text{La}_{0.4}\text{CuO}_{6+\delta}$ (open circles), $\text{Bi}_2\text{Sr}_{1.7}\text{La}_{0.3}\text{CuO}_{6+\delta}$ (open squares), and $\text{Bi}_{1.8}\text{Pb}_{0.3}\text{Sr}_2\text{Ca}_{0.9}\text{Cu}_2\text{O}_{8+\delta}$ (open diamonds) have a T_c maximum as the number of dopant holes, x_p , decreases. For

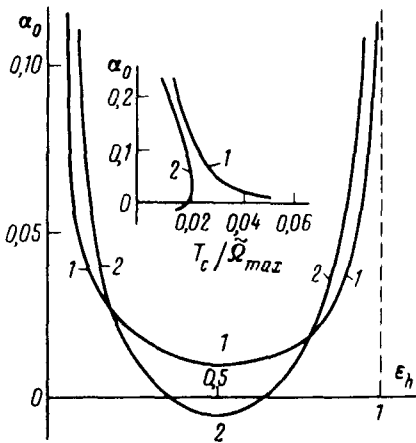


FIG. 3.

$\text{YBa}_2\text{Cu}_3\text{O}_{7-\delta}$ (crosses), we find a maximum as x_p increases. The solid curve in Fig. 4 is a plot of $T_c(x_p)$ for $\text{La}_{2-x}\text{Sr}_x\text{CuO}_4$ [we are ignoring the dip in T_c in the region of structural instability, $x \approx 0.13$ (Refs. 14–16)].

4. Comparing the theoretical results on $T_c(\mathcal{E}_h)$ in Fig. 2 with the experimental results on $T_c(x_p)$ in Fig. 4, we see that the plasmon mechanism for high- T_c superconductivity gives a qualitatively correct description of the behavior as a function of the parameters of both the nearly symmetric bell-shaped curves of T_c versus x_p or x_n for $\text{La}(\text{BaSr})\text{CuO}$ or NdCeCuO (Refs. 1–5) (see solid curve 1 in Fig. 2) and the broad plateau on the $T_c(x_p)$ curves for the mixed cuprates YBaLaCuO (124), BiPbSrCaCuO (2223), and TlPbSrCaYCuO (1212) (see the dashed curve in Fig. 2). The asymmetric curves of $T_c(x_p)$, with a maximum, for BiPbSrLaCuO (2201), BiSrLaCuO (2201), BiPbSrCaCuO (2212), and YBaCuO (123) can be compared with either the right-hand or left-hand maximum on double-humped theoretical curve 2 in Fig. 2 over a limiting interval of variation (decrease or increase) in the density of dopant holes, when there is an increase in the number of h electrons or h holes in the

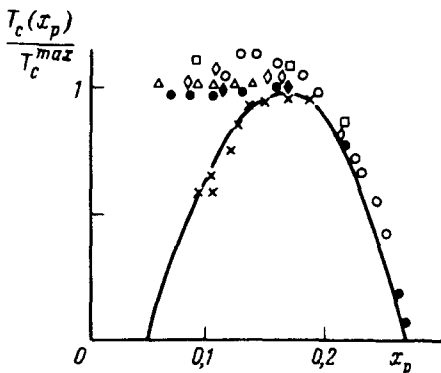


FIG. 4.

narrow band. We note in this connection that the experimental data in Ref. 1 for BiSrCaCuO (2223) doped with Na and K indicate that T_c goes through a minimum and then increases with increasing x_p . This result, combined with the negative value found in Ref. 9 for the oxygen isotope-effect exponent ($\alpha_0 < 0$) in Bi_{1.6}Pb_{0.4}Sr₂Ca₂Cu₃O₁₀, is evidence of the possible observation in this class of compounds of a double-humped T_c curve over a broad range of x_p , like curve 2 in Fig. 2, which corresponds to curves 2 in Fig. 3, with negative values of α_0 near the T_c maximum at a half-filled narrow 2D band ($\mathcal{E}_h = 0.5$).

The general tendency for the oxygen isotope-effect exponent to decrease (increase) with increasing (decreasing) transition temperature, as is shown by the inset in Fig. 3, and as is characteristic of the plasmon mechanism of high- T_c superconductivity,¹² agrees qualitatively with experimental data on various cuprates,^{7,8,9,11} including the negative values of α_0 in YBaSrCuO (123) (Ref. 8) and in BiPbSrCaCuO (2223) (Ref. 9).

At the same time, the curve of $\alpha_0(x)$ in La_{2-x}Sr_xCuO₄ (Ref. 13) is masked to a large extent by effects stemming from the pronounced anharmonicity of the phonons near the point of the structural instability of the lattice ($x = 0.13$). Still, it correlates with theoretical curve 1 in Fig. 3 at $\mathcal{E}_h > 0.5$ over the entire region of the decrease in T_c ($x > 0.15$), except in a narrow neighborhood of the point $x \approx 0.27$, in which we find $T_c \rightarrow 0$. However, it should be kept in mind that the sharp increase in α_0 near the boundaries of the narrow 2D band at the points $\mathcal{E}_h = 0$ and $\mathcal{E}_h = 1$ (Fig. 3) may not be seen experimentally, because of an inhomogeneous composition (oxygen content) in the interior of the samples and because of the corresponding scatter in the values of the local hole density.

In addition, the superconductivity with low values, $T_c < 5$ K, which was observed in Ref. 16 in the lightly doped cuprate La_{1.98}(Ce, K)_{0.02}Ba_xCuO₄ at $x < 0.05$ agrees with the nonvanishing value of T_c at $\mathcal{E}_h = 0$ (Fig. 2) due to an electron-phonon coupling in the absence of an electron-plasmon coupling, with $\Omega_h = 0$ as $T \rightarrow 0$ but $\tilde{\Omega} \neq 0$ (Fig. 1).

5. All the characteristic features of the density dependence of T_c and α_0 in the cuprates can thus be explained at a qualitative level by the model of a plasmon mechanism for high- T_c superconductivity.¹² A more reliable quantitative comparison of theory and experiment will require more-comprehensive and more-accurate measurements of T_c and α_0 as a function of x_p (or x_h) in the same samples, over a range of the density of dopant holes (or dopant electrons) as wide as possible. Of considerable interest in this connection are the new mercury-based layered cuprates which were recently discovered with the Hg (1201) and Hg (1212) structures, with $T_c \approx 35$ –94 K, and Hg (1223) structures, with $T_c \approx 133$ –140 K.^{22,23} In these compounds, there is actually a complete replacement of Tl by Hg, with a lower valence. As a result, under otherwise equal conditions (in particular, at a fixed oxygen saturation), the hole densities are higher; according to the theoretical conclusions of Ref. 12 and the experiments of Refs. 21–23, the values of T_c are higher in this “overdoped” compound. In Hg (1223), however, T_c is observed to increase with increasing applied pressure P ($dT_c/dP > 0$) after synthesis. In other words, this compound is

“underdoped.”²² This contradiction can be resolved by assuming that the initial states of the mercury compounds with relatively high hole densities correspond to the left-hand (ascending) branch of the right-hand maximum on the double-humped curve of T_c versus x_p (see curve 2 in Fig. 2). Here one should observe a negative oxygen isotope effect ($\alpha_0 < 0$). Testing this suggestion will require measuring $T_c(x_p)$ and $\alpha_0(x_p)$ for these cuprates and also for the mixed-composition compounds $Tl_{1-x}Hg_xBa_2Ca_{n-1}Cu_nO_y$ over a broad range of the hole density.

I wish to thank V. M. Pan, V. I. Pentegov, and A. V. Semenov for useful discussions of the experimental results and certain theoretical aspects of this problem.

- ¹J. B. Torrance, A. Bezing, A. I. Nazzari *et al.*, *Physica C* **162–164**, 291 (1989).
- ²S. Uchida, *Physica C* **185–189**, 28 (1991).
- ³J. L. Tallon, R. G. Buckley, E. M. Haines *et al.*, *Physica C* **185–189**, 855 (1991).
- ⁴T. Fujita, Y. Aoki, Y. Maeno *et al.*, *Jpn. J. Appl. Phys.* **26**, L368 (1987).
- ⁵Y. Tokura, H. Takagi, and S. Uchida, *Nature* **337**, 345 (1989).
- ⁶J. H. Brewer, E. J. Ashaldo, J. F. Carolan *et al.*, *Phys. Rev. Lett.* **60**, 1073 (1988).
- ⁷J. P. Frank, J. Jang, M. A.-K. Mohamed *et al.*, *Phys. Rev. B* **44**, 5318 (1991).
- ⁸H. J. Bornemann and D. E. Morris, *Phys. Rev. B* **44**, 5322 (1991).
- ⁹H. J. Bornemann, D. E. Morris, and H. B. Liu, *Physica C* **182**, 132 (1991).
- ¹⁰P. Morel and P. W. Anderson, *Phys. Rev.* **125**, 1263 (1962).
- ¹¹P. B. Allen, *Nature* **335**, 258 (1988).
- ¹²É. A. Pashitskii, *JETP Lett.* **55**, 300 (1992); **56**, 405 (1992); *Zh. Eksp. Teor. Fiz.* **103**, 867 (1993) [*JETP* **76**, 425 (1993)].
- ¹³M. K. Crawford, W. E. Farneth, R. Miao *et al.*, *Physica C* **162–164**, 755 (1989).
- ¹⁴A. R. Moodenbaugh, Y. Xu, M. Suenaga *et al.*, *Phys. Rev. B* **38**, 4596 (1988).
- ¹⁵H. Takagi, T. Ido, S. Ishibashi *et al.*, *Phys. Rev. B* **40**, 2254 (1989).
- ¹⁶Y. Koike, T. Kawaguchi, S. Hosoya *et al.*, *Physica C* **185–189**, 791 (1991).
- ¹⁷É. A. Pashitskii, Yu. M. Malozovskii, and A. V. Semenov, *Zh. Eksp. Teor. Fiz.* **100**, 465 (1991) [*Sov. Phys. JETP* **73**, 255 (1991)]; *Ukr. Fiz. Zh.* **36**, 889 (1991); *Supercon. Sci. Technol.* **5**, 507 (1992).
- ¹⁸M. Suzuki, *Phys. Rev. B* **39**, 2312 (1989).
- ¹⁹H. Romberg, M. Alexander, N. Nucker *et al.*, *Phys. Rev. B* **42**, 8768 (1990).
- ²⁰É. A. Pashitskii, *JETP Lett.* **57**, 648 (1993).
- ²¹S. N. Putilin, E. V. Antipov, O. Chmaissem *et al.*, *Nature* **362**, 226 (1993).
- ²²A. Schilling, M. Cantoni, J. D. Cuo *et al.*, *Nature* **363**, 56 (1993).
- ²³L. Gao, J. Z. Huang, R. L. Meng *et al.*, *Physica C*, to be published (1993).

Translated by D. Parsons